IRIS AperTO

UNIVERSITÀ DEGLI STUDI DI TORINO

AperTO - Archivio Istituzionale Open Access dell'Università di Torino

Wavelet analysis of a Cu-oxo zeolite EXAFS simulated spectrum

This is the author's manuscript

Original Citation:

Availability:

This version is available http://hdl.handle.net/2318/1768589 since 2021-01-23T12:41:20Z

Published version:

DOI:10.1016/j.radphyschem.2019.05.023

Terms of use:

Open Access

Anyone can freely access the full text of works made available as "Open Access". Works made available under a Creative Commons license can be used according to the terms and conditions of said license. Use of all other works requires consent of the right holder (author or publisher) if not exempted from copyright protection by the applicable law.

(Article begins on next page)

07 January 2023

IRIS AperTO

UNIVERSITÀ DEGLI STUDI DI TORINO

This is the author's final version of the contribution published as:

Martini A.; Pankin I.A.; Marsicano A.; Lomachenko K.A.; Borfecchia E., Wavelet analysis of a Cu-oxo zeolite EXAFS simulated spectrum. Rad. Phys. Chem., 175, 2020, 108333.

DOI: 10.1016/j.radphyschem.2019.05.023

The publisher's version is available at:

https://www.sciencedirect.com/science/article/pii/S0969806X18309551

When citing, please refer to the published version.

Link to this full text:

http://hdl.handle.net/2318/1768589

iris-AperTO

University of Turin's Institutional Research Information System and Open Access Institutional Repository

Wavelet Analysis of a Cu-oxo zeolite EXAFS simulated spectrum

Andrea Martini[1,2,*], Ilia A. Pankin[1,2], Anna Marsicano[3], Kirill A. Lomachenko[4], ElisaBorfecchia[5]

[1] *Department of Physics, CrisDi Interdepartmental Center, University of Turin, via P. Giuria 1, 10125 Turin, Italy.*
[2] *Smart Materials, Research Institute, Southern Federal University, Sladkova Street 174/28, 344090 Rostov-on-Don, Russia.*
[3] *Institut Charles Gerhardt Montpellier, UMR5253 CNRS-UM-ENSCM, Université de Montpellier, Place Eugène Bataillon, 340957 Montpellier Cedex 5, France*
[4] *European Synchrotron Radiation Facility, 71 avenue des Martyrs, CS 40220, 38043 Grenoble Cedex 9, France.*

[5] *Center for Materials Science and Nanotechnology (SMN), Department of Chemistry, University of Oslo, 1033 Blindern, 0315 Oslo, Norway.*

(*) Corresponding Author: andrea.martini@unito.it

Abstract

In this work, we focus on the simulated EXAFS spectrum of a Cu-oxo dimer sited in the eight-membered ring of the chabazite zeolite framework. We show the high level of complexity related to the analysis of the second and third shell of the EXAFS-Fourier transform due to the overlap of contributions stemming from atomic species present in the Cu-local environment. Subsequently, we demonstrate the potential of Wavelet Transform Analysis as a new tool in the identification and visualization of EXAFS atomic contributions, providing an easier and effective interpretation of the data collected on Cu-zeolite systems.

Keywords:

Wavelet Transform Analysis, EXAFS, Direct CH_4 to CH_3OH conversion, Cu-exchanged chabazite.

1. Introduction

Cu-exchanged zeolites, in particular Cu-chabazite (Cu-CHA) and Cu-mordenite (Cu-MOR), have been proven to possess the active sites able to cleave the C-H bond of methane, enabling methane's direct partial oxidation to methanol (MTM) (Pappas et al., 2017; Wulfers et al., 2015). Clearly, the key to understanding the reliability and the potentiality of this material for the MTM process lies in a detailed characterization of the Cu-speciation during O_2 activation, when Cu active sites are formed. It is worth noting that Cu moieties that are held to be active sites for one zeolite framework are not always held to be active sites for other topologies. Nevertheless, the experimental XAS data of the two types of zeolites, CHA and MOR, demonstrated that there were no sharp differences in the activated state, and the behaviour observed for all the investigated samples along the step-wise process was rather similar (Alayon et al., 2014; Pappas et al., 2017). However, the interpretation of the EXAFS signal significantly differs for the two topologies. While the first peak of the EXAFS Fourier transform (FT-EXAFS) is commonly associated to Cu-O single scattering paths (SS), the interpretation of the second peak seems to be more uncertain. We simulated an EXAFS spectrum referring to a mono-(μ-oxo) dicopper(II) species sited in CHA eight membered ring (8r) (see Figure 1a) proposed as one of the plausible Cu active sites for MTM (Chen et al., 2018). Here we used Wavelet Transform Analysis (WTA) in order to demonstrate the potential of this technique in the discrimination of different atomic contributions that could be difficult to resolve in an unambiguous way from the traditional Fourier Transform analysis of the EXAFS spectrum.

2. Methods.

2.1. Wavelet Transform of an EXAFS spectrum.

Given a molecular structure, the easiest way to evaluate the interatomic distances R (direct space), of certain atoms around a determined absorber, consists in performing a spectral analysis of the related EXAFS signal $\chi(k)$ (Mino et al., 2013; Stern, 1974) using the Fourier Transform (FT). However, if two groups of different atoms are localized differently at close distances, their contributions in R-space overlap, becoming indistinguishable (Timoshenko and Kuzmin, 2009). It is possible to see that the backscattering-amplitude factor presents a strong dependence on the atomic number Z: heavy atoms have large values of the atomic backscattering amplitude $F_i(k)$ at high wavenumbers whereas light atoms at low k-values. As a result, their contributions into the total EXAFS signal are differently localized in the k-space (Soldatov et al., 2018). Herein, this evidence can be used for signal discrimination obtaining a two-dimensional representation of the EXAFS spectrum with a simultaneous signal localization in k and R space. To this purpose, Wavelet Transform (WT) of the k^n-weighted EXAFS spectrum can be applied. It is described by the following two-dimensional integral transform:

$$w(a,b) = \frac{1}{\sqrt{a}} \int_{-\infty}^{+\infty} dk'\, k'^{n} \chi(k') \psi^{*}\left(\frac{k'-b}{a}\right) \quad (1)$$

This equation can be seen as the inner product between the analysed spectrum $\chi(k)$ and a defined window function ψ, called "mother wavelet" or simply wavelet (where the apex ψ^{*} denotes the complex conjugate of ψ), which must decay at zero for higher values of $|k'|$ (Funke et al., 2005). Here, the signal $\chi(k)$ is analysed through a set of train-waves (wavelets) that are shifted by b units in the k-space and distorted by a factor a in order to take account of the local frequencies of the signal (Soldatov et al., 2018). The variables a and b are connected to the k and R-space by the following relations: $b = k$ and $a = \eta/2R$. The description of the parameter η will be given below.

In our study, we compared the results obtained from two different window functions applied on the same theoretical EXAFS spectrum: the Morlet and Cauchy wavelet (Funke et al., 2005; Munoz et al., 2003; Penfold et al., 2013; Soldatov et al., 2018; Timoshenko and Kuzmin, 2009). The first one is characterized by a fast oscillatory part localized by a Gaussian envelope, making its real and imaginary part similar to an EXAFS spectrum: $\psi_{\eta,\sigma}(k) = \frac{1}{\sqrt{2\pi\sigma}} \exp(i\eta k) \exp(-k^2/2\sigma^2)$. Here the parameter η represents the frequency of sine and cosine waves while σ corresponds to the Gaussian standard deviation. Both parameters must be chosen accurately because of their basic role in the signal resolution in k and R spaces. It is worth mentioning that the WT distributes the signal information The second window function used over k-R cells that are often referred to as Heisenberg boxes (Funke et al., 2005; Penfold et al., 2013). On this basis, it is possible to demonstrate that the resolutions in k and R-space are inversely proportional (*i.e.* good resolution in k-space implies a loss of information in R-space and vice versa). is the Cauchy wavelet. It is represented by the following equation: $\psi_{\eta}(k) = (i/(k+i))^{\eta+1}$(where i denotes the complex unit). By choosing this window function, it is possible to simplify the integral of equation (1). Moreover the usage of a complex-valued function seems to be well suitable for analysing frequency-modulated signals (Munoz et al., 2003). With respect to the resolution, the same considerations made for the Morlet wavelet remain valid (Soldatov et al., 2018). However the resolution is controlled here by just one parameter: (η) instead of two (η, σ).

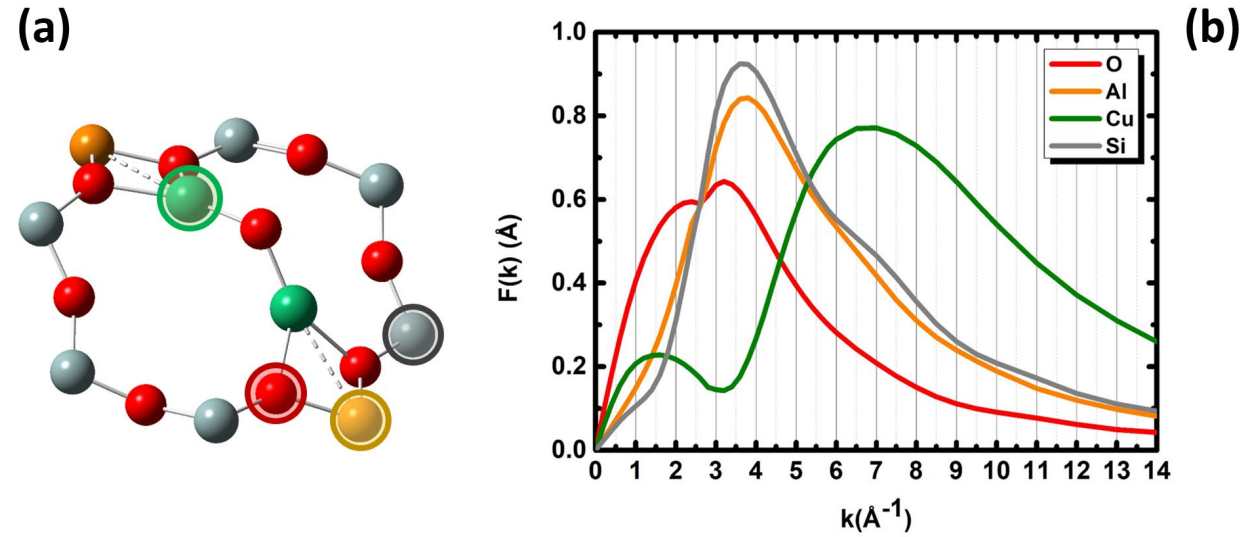

Figure 1: (a) DFT optimized structure of a mono-(μ-oxo) dicopper (II) species inserted in the 8r of CHA framework. (b) Plot of the backscattering amplitude factor multiplied for a k^0 value. Each $F_i(k)$ term presented in the graph refers to the Cu-SS path with the atoms indicated with the coloured circles in (a).

2.2. DFT-assisted EXAFS simulation procedure.

We performed the EXAFS simulation of the DFT optimized-geometry (optimization has been performed using plane wave basis set and PBE pseudopotential (Kresse and Joubert, 1999) approach as implemented in the VASP 5.3 code (Kresse and Furthmuller, 1996)) reported in Figure 1a. Phase and amplitudes have been calculated by FEFF6 code using Arthemis software from the Demeter package (Ravel and Newville, 2005). Herein, we consider all paths up to 4 Å with a scattering amplitude higher than 15% if compared to the stronger one that is the single-scattering (SS) path with the first shell represented by the bridging oxygen atom. Using this cut off, only SS paths have been included in the model, being the amplitude of the stronger multiple scattering (MS) path of 12%. The structural parameters (*i.e.* coordination number N_i and bond distances R_i) for all the included shell were set to the DFT values. The Debye Waller (DW) parameters have been chosen for each shell according on the types of atoms and their distances from the absorber, this done on the basis of some recent experimental work conducted on this topic (Borfecchia et al., 2015; Pappas et al., 2017). We fixed, for the extra-framework oxygen (O_efw), a DW parameters to 0.005 $Å^2$ .The same value has been used to describe the

contributions involving the second sub-shell of framework oxygens (O_fw). Subsequently, we set the DW factor, related to the Al site shell, to 0.008 Å^2. The same DW factor was fixed for the Cu site too.
For the framework atoms, we employed a lower level parametrization strategy for the O and Si atoms that compose the zeolite framework, providing a minor but not negligible contribute to the EXAFS signal. We assigned a DW factor defined in the following way: $\sigma^2 = \sigma_{fw}^2 \cdot \sqrt{R_i/R_T}$, where σ_{fw}^2 has been fixed to a global value of 0.01 Å^2, R_i is the position of the O or Si atoms in the zeolite ring, while the term R_T represents the distance of the nearest framework atom from the Cu site that has been parametrized following this procedure. This choice seems appropriate; in fact, it provides a slow increasing of the DW factor as the distance increases (isotropic increasing), keeping account of the structural variation or thermal motion typically more pronounced at higher distances (Sevillano et al., 1979). Finally, we set the amplitude factor S_0 and the threshold energy to 1 (ideal value for S_0) and 0 eV (no spectrum energy shifting) respectively. The entire parametrization procedure, described above, has been applied for each Cu site in the dicopper species separately, considering the same shell subdivisions. Consequently, the simulated final spectrum was obtained by averaging the two total spectra retrieved from each Cu atom chosen as absorber. Thus, we were able to reproduce a reasonable "theoretical" EXAFS spectrum from the DFT optimized structure. Concomitantly, we could ascertain the contribution of each shell of Cu-atomic neighbours from the total EXAFS signal, as it is possible to see from Figure 2a.

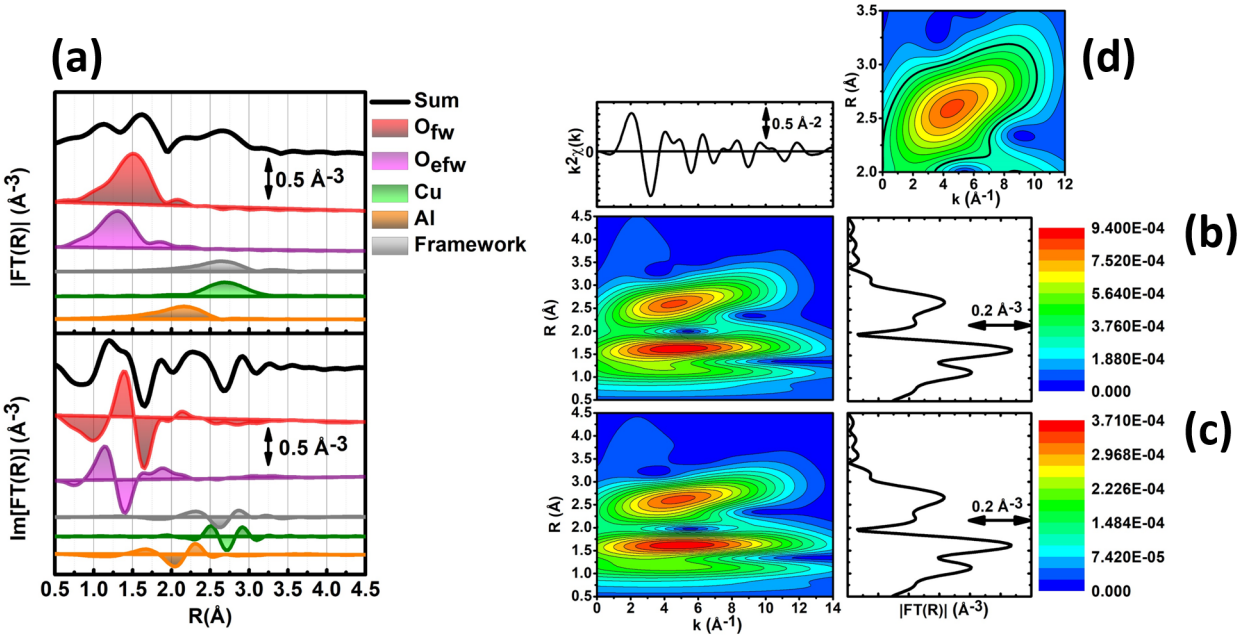

Figure 2: (a) Magnitude and Imaginary part of the phase uncorrected FT-EXAFS signal calculated starting from the structure reported in Figure 1(a). For the FT signal calculation an hanning type apodization window (Δk=2.4 -11 Å^{-1}; dk=1) has been used on a k^2 multiplied $\chi(k)$. We chose a k-range defined in this way in order to reproduce an EXAFS signal as similar as possible to experimental spectra, previously reported in ref. (Pappas et al., 2017). (b),(c) Morlet ($\sigma = 1$, $\eta = 12$)and Cauchy ($\eta = 200$) wavelet transforms of the simulated EXAFS signal. (d) Magnification of the Cauchy WT third lobe. The black contour line emphasizes the presence of two sub-lobes localized at low and high k-values. In particular, this last feature is associated to the presence of the Cu-Cu path.

3. Result and Discussions

The magnitude and the imaginary part analysis of each contribute related to the total simulated signal allows us to obtain deeper insights into the FT peak assignment. Analysing Figure 2a it is possible to clearly distinguish two main peaks, arising from SS involving first- and second-shell atomic neighbours, respectively. The first-shell peak is further structured into two different contributions. The first one, less intense, is due to the extra framework oxygen (violet line) while the second peak (red line), much more intense, depends on the averaged contribution of the two framework oxygens coordinated to the Cu site. It is interesting to observe how the O_efw imaginary part contribution compensates the O_fw one, reducing the global magnitude of the first-shell peak. Significantly, the Al site takes part in the total spectra in the second shell (orange line). Seemingly, the framework atoms (grey line) contribute in the second shell too. The phase-uncorrected FT of the simulated EXAFS spectrum shows the Cu-Cu contribute peaking at ca. 2.8 Å (green line) and extending in the range between 2.4 and 3.5 Å. Globally, Cu peaks are always more intense than the ones due to the framework signals; however, the much lower coordination number (N_{Cu} =1) and the rather long Cu-Cu distances render these metal-metal contributions much weaker than what is observed in the bulk Cu-metal or Cu-oxide references. It follows that, from the simulated FT-EXAFS spectrum, we are not able to appreciate the principal feature coming from Cu-Cu contribution that lies in the second shell region and at these distances the Cu signal intensity decreases significantly. Under these conditions, WTA seems to be the only way we can ascertain the presence of a Cu-dimer geometry. In Figure 2b,c are reported two WTs applied to the same theoretical EXAFS signal: Figure 2b: Morlet wavelet, Figure 2c: Cauchy wavelet. Globally, neither wavelet shows a huge difference from the other in spectral-features

representations, apart from the wavelet magnitude, which is higher for the Morlet wavelet. However, this phenomenon depends exclusively on the functional form of the wavelet used. For all the wavelet representations, we can recognize two lobes localized at low R values ΔR=(1-1.5 Å) in the direct space. They can be clearly associated to the Cu-O_efw and Cu-O_fw, respectively. Nevertheless, the lobes maxima tend to be stretched in the k-space towards high k-values (around 9 $Å^{-1}$). This region is typically populated by atoms heavier than oxygen. However, the reason for this particular behaviour must be found in the so-called *broadening effect*. It is a general problem of WTA and it is not only restricted to the Morlet and Cauchy wavelets (Timoshenko and Kuzmin, 2009). There is a third lobe that extends in both wavelets between ΔR=(2-3.5 Å) and Δk=(0.5-11 $Å^{-1}$), as we can see from the magnification reported in Figure 2c. Analysing it in details, it is possible to observe that it is composed by the union of two sub-lobes. The first sub-lobe develops in the k-range between Δk =(0.5-6 $Å^{-1}$). It is possible to confirm that it is generated by the contribution of framework oxygens (low k-contributes) and by Si and Al, whose backscattering amplitude factor peaks in the k-space around 4 $Å^{-1}$. Having a comparable Z, the features related to Si and Al atoms can not be identified through WTA. The second sub-lobe extends between Δk =(6-11 $Å^{-1}$). The maximum of the Cu backscattering amplitude falls within this range and this is the main reason for the sub-lobe shifting towards high k-values. However, the FT analysis illustrates that, where the Cu-Cu peak is present in the R region, the Si/O framework contributions overlap the Cu shell. In particular, the Si (SS) path is characterized by a backscattering amplitude factor that is lower in magnitude at high k-values than the factor of the Cu, but it is not negligible (see Figure 1b). This is the main reason why the Cu sub-lobe is not completely separated from the Al, Si and O sub-lobes, making its complete resolution impossible to realise.

4. Conclusions and perspectives

We applied the WTA analysis on a theoretical signal obtained starting from a DFT optimized Cu-dimer structure sited in the CHA (8r). The analysis of the EXAFS-FT showed the complexity associated with the peak assignment because of the overlapping contributions of the different shells of scatterers (O, Si, Al and Cu) sited around the absorber. Here, the application of WTA showed how it is possible to overcome this problem leading to clearer identification of the Cu-Cu contribution. The next step of our study will take advantage of the higher sensitivity to the scatterer nature, proper of the wavelet representation, to perform fits of experimental data, as already done in the pioneering work of Kuzmin and co-workers (Jonane et al., 2018; Jonane et al., 2016; Timoshenko et al., 2015; Timoshenko et al., 2014a; Timoshenko et al., 2012, 2014b).At present, the major difficulty in applying this approach consists in the heterogeneity of Cu species present in the real zeolite-based catalysts (i.e. different Cu-monomers and dimers can coexist) and in their relative concentration as a function of the pre-treatment and process conditions (Borfecchia et al., 2015; Lomachenko et al., 2016; Martini et al., 2018; Martini et al., 2017; Pappas et al., 2017; Pappas et al., 2018).
Globally, the results highlight that WT approach could represent a more promising technique than conventional FT, both for the visualization and the interpretation of theoretical and experimental EXAFS signals, permitting to discriminate contributions from heavy and light scatterers in the Cu local environment in zeolite-based catalysts, thus shedding light on the long-standing question about nuclearity of Cu-oxo species formed in these materials after high-temperature activation in O_2.

Acknowledgements
AM and IAP acknowledge support from the project “Department of Excellence” (L. 232/2016), founded by the Italian Ministry of Education, University and Research (MIUR). AM and IAP acknowledge the Megagrant of the Russian Federation Government to support scientific research at the Southern Federal University, No.14.Y26.31.0001. We are grateful to Professor C. Lamberti (University of Turin) for insightful discussions and advices.

References

Alayon, E.M.C., Nachtegaal, M., Bodi, A., van Bokhoven, J.A., 2014. Reaction Conditions of Methane-to-Methanol Conversion Affect the Structure of Active Copper Sites. ACS Catal. 4, 16-22.
Borfecchia, E., Lomachenko, K., Giordanino, F., Falsig, H., Beato, P., Soldatov, A., Bordiga, S., Lamberti, C., 2015. Revisiting the nature of Cu sites in the activated Cu-SSZ-13 catalyst for SCR reaction. Chem. Sci. 6, 548-563.
Chen, L., Falsig, H., Janssens, T.V.W., Jansson, J., Skoglundh, M., Gronbeck, H., 2018. Effect of Al-distribution on oxygen activation over Cu-CHA. Catal. Sci. Technol. 8, 2131-2136.
Funke, H., Scheinost, A.C., Chukalina, M., 2005. Wavelet analysis of extended x-ray absorption fine structure data. Phys. Rev. B 71, 7.
Jonane, I., Anspoks, A., Kuzmin, A., 2018. Advanced approach to the local structure reconstruction and theory validation on the example of the W L-3-edge extended x-ray absorption fine structure of tungsten. Model. Simul. Mater. Sci. Eng. 26, 11.
Jonane, I., Timoshenko, J., Kuzmin, A., 2016. Atomistic simulations of the Fe K-edge EXAFS in FeF3 using molecular dynamics and reverse Monte Carlo methods. Phys. Scr. 91, 6.
Kresse, G., Furthmuller, J., 1996. Efficiency of ab-initio total energy calculations for metals and semiconductors using a plane-wave basis set. Comput. Mater. Sci. 6, 15-50.

Kresse, G., Joubert, D., 1999. From ultrasoft pseudopotentials to the projector augmented-wave method. Phys. Rev. B 59, 1758-1775.
Lomachenko, K.A., Borfecchia, E., Negri, C., Berlier, G., Lamberti, C., Beato, P., Falsig, H., Bordiga, S., 2016. The Cu-CHA deNO(x) Catalyst in Action: Temperature-Dependent NH3-Assisted Selective Catalytic Reduction Monitored by Operando XAS and XES. J. Am. Chem. Soc. 138, 12025-12028.
Martini, A., Alladio, E., Borfecchia, E., 2018. Determining Cu-Speciation in the Cu-CHA Zeolite Catalyst: The Potential of Multivariate Curve Resolution Analysis of In Situ XAS Data. Top. Catal. 61, 1396-1407.
Martini, A., Borfecchia, E., Lomachenko, K.A., Pankin, I.A., Negri, C., Berlier, G., Beato, P., Falsig, H., Bordiga, S., Lamberti, C., 2017. Composition-driven Cu-speciation and reducibility in Cu-CHA zeolite catalysts: a multivariate XAS/FTIR approach to complexity. Chem. Sci. 8, 6836-6851.
Mino, L., Agostini, G., Borfecchia, E., Gianolio, D., Piovano, A., Gallo, E., Lamberti, C., 2013. Low-dimensional systems investigated by x-ray absorption spectroscopy: a selection of 2D, 1D and 0D cases. J. Phys. D-Appl. Phys. 46, 72.
Munoz, M., Argoul, P., Farges, F., 2003. Continuous Cauchy wavelet transform analyses of EXAFS spectra: A qualitative approach. Am. Miner. 88, 694-700.
Pappas, D.K., Borfecchia, E., Dyballa, M., Pankin, I.A., Lomachenko, K.A., Martini, A., Signorile, M., Teketel, S., Arstad, B., Berlier, G., Lamberti, C., Bordiga, S., Olsbye, U., Lillerud, K.P., Svelle, S., Beato, P., 2017. Methane to Methanol: Structure–Activity Relationships for Cu-CHA. J. Am. Chem. Soc. 139, 14961–14975.
Pappas, D.K., Martini, A., Dyballa, M., Kvande, K., Teketel, S., Lomachenko, K.A., Baran, R., Glatzel, P., Arstad, B., Berlier, G., Lamberti, C., Bordiga, S., Olsbye, U., Svelle, S., Beato, P., Borfecchia, E., 2018. The Nuclearity of the Active Site for Methane to Methanol Conversion in Cu-Mordenite: A Quantitative Assessment. J. Am. Chem. Soc. 140, 15270-15278.
Penfold, T.J., Tavernelli, I., Milne, C.J., Reinhard, M., El Nahhas, A., Abela, R., Rothlisberger, U., Chergui, M., 2013. A wavelet analysis for the X-ray absorption spectra of molecules. J. Chem. Phys. 138, 7.
Ravel, B., Newville, M., 2005. ATHENA, ARTEMIS, HEPHAESTUS: data analysis for X-ray absorption spectroscopy using IFEFFIT. J. Synchrot. Radiat. 12, 537-541.
Sevillano, E., Meuth, H., Rehr, J.J., 1979. Extended x-ray absorption fine structure Debye-Waller factors. I. Monatomic crystals. Phys. Rev. B 20, 4908-4911.
Soldatov, M.A., Martini, A., Bugaev, A.L., Pankin, I., Medvedev, P.V., Guda, A.A., Aboraia, A.M., Podkovyrina, Y.S., Budnyk, A.P., Soldatov, A.A., Lamberti, C., 2018. The insights from X-ray absorption spectroscopy into the local atomic structure and chemical bonding of Metal–organic frameworks. Polyhedron 155, 232-253.
Stern, E.A., 1974. Theory of the extended x-ray-absorption fine structure. Phys. Rev. B 10, 3027-3037.
Timoshenko, J., Anspoks, A., Kalinko, A., Jonane, I., Kuzmin, A., 2015. Local Structure of Multiferroic MnWO4 and Mn0.7Co0.3WO4 Revealed by the Evolutionary Algorithm. Ferroelectrics 483, 68-74.
Timoshenko, J., Anspoks, A., Kalinko, A., Kuzmin, A., 2014a. Analysis of extended x-ray absorption fine structure data from copper tungstate by the reverse Monte Carlo method. Phys. Scr. 89, 6.
Timoshenko, J., Kuzmin, A., 2009. Wavelet data analysis of EXAFS spectra. Comput. Phys. Commun. 180, 920-925.
Timoshenko, J., Kuzmin, A., Purans, J., 2012. Reverse Monte Carlo modeling of thermal disorder in crystalline materials from EXAFS spectra. Comput. Phys. Commun. 183, 1237-1245.
Timoshenko, J., Kuzmin, A., Purans, J., 2014b. EXAFS study of hydrogen intercalation into ReO3 using the evolutionary algorithm. J. Phys.-Condes. Matter 26, 15.
Wulfers, M.J., Teketel, S., Ipek, B., Lobo, R.F., 2015. Conversion of methane to methanol on copper-containing small-pore zeolites and zeotypes. Chem. Commun. 51, 4447-4450.